CUE-101, a Novel E7-pHLA-IL2-Fc Fusion Protein, Enhances Tumor Antigen-Specific T-Cell Activation for the Treatment of HPV16-Driven Malignancies

Steven N. Quayle[1], Natasha Girgis[1], Dharma R. Thapa[1], Zohra Merazga[1], Melissa M. Kemp[1], Alex Histed[1], Fan Zhao[1], Miguel Moreta[1], Paige Ruthardt[1], Sandrine Hulot[1], Alyssa Nelson[1], Lauren D. Kraemer[1], Dominic R. Beal[1], Luke Witt[1], Jessica Ryabin[1], Jonathan Soriano[1], Mark Haydock[1], Emily Spaulding[1], John F. Ross[1], Peter A. Kiener[2], Steven Almo[3], Rodolfo Chaparro[1], Ronald Seidel[1], Anish Suri[1], Saso Cemerski[1], Kenneth J. Pienta[4], and Mary Ellen Simcox[1]

ABSTRACT

Purpose: To assess the potential for CUE-101, a novel therapeutic fusion protein, to selectively activate and expand HPV16 $E7_{11-20}$-specific $CD8^+$ T cells as an off-the shelf therapy for the treatment of HPV16-driven tumors, including head and neck squamous cell carcinoma (HNSCC), cervical, and anal cancers.

Experimental Design: CUE-101 is an Fc fusion protein composed of a human leukocyte antigen (HLA) complex, an HPV16 E7 peptide epitope, reduced affinity human IL2 molecules, and an effector attenuated human IgG1 Fc domain. Human E7-specific T cells and human peripheral blood mononuclear cells (PBMC) were tested to demonstrate cellular activity and specificity of CUE-101, whereas *in vivo* activity of CUE-101 was assessed in HLA-A2 transgenic mice. Antitumor efficacy with a murine surrogate (mCUE-101) was tested in the TC-1 syngeneic tumor model.

Results: CUE-101 demonstrates selective binding, activation, and expansion of HPV16 $E7_{11-20}$-specific $CD8^+$ T cells from PBMCs relative to nontarget cells. Intravenous administration of CUE-101 induced selective expansion of HPV16 $E7_{11-20}$-specific $CD8^+$ T cells in HLA-A2 (AAD) transgenic mice, and anticancer efficacy and immunologic memory was demonstrated in TC-1 tumor-bearing mice treated with mCUE-101. Combination therapy with anti-PD-1 checkpoint blockade further enhanced the observed efficacy.

Conclusions: Consistent with its design, CUE-101 demonstrates selective expansion of an HPV16 $E7_{11-20}$-specific population of cytotoxic $CD8^+$ T cells, a favorable safety profile, and *in vitro* and *in vivo* evidence supporting its potential for clinical efficacy in an ongoing phase I trial (NCT03978689).

Introduction

Oncogenic human papilloma virus (HPV) is responsible for many cervical and anal cancers and head and neck squamous cell carcinoma (HNSCC; refs. 1, 2). Approximately 70% to 80% of HPV-driven oropharyngeal cancers in the United States are HPV16/18 driven, and their incidence continues to rise (3, 4). Prophylactic HPV vaccines have no therapeutic effect on established disease, thus HPV infections are expected to continue contributing to the global cancer burden (5). Recent studies suggest that HPV^+ cancers may be successfully targeted with T-cell therapy, wherein adoptive transfer of tumor-infiltrating or genetically engineered T cells was shown to induce responses in HPV-associated cancer patients (6–8). These studies provide proof of concept that a therapeutic strategy that increases the frequency of tumor antigen specific T cells may be sufficient to drive clinical benefit in this population.

HPV16 E7 is constitutively expressed in HPV-associated cancers, is necessary for both initiation and maintenance of malignant transformation, and is genetically conserved in cancer with essentially no variation in sequence among isolates of precancerous and cancerous lesions in subjects from around the world (9). Importantly, the $E7_{11-20}$ peptide is maintained in cancer, is an immunodominant CD8 epitope in humans, and is one of the E7 epitopes identified with relatively high affinities for HLA-A*0201, which is expressed in approximately 40% to 50% of people of European descent (10–12). Although the E7 oncoprotein is a promising target for therapy of HPV-driven cancers, HPV driver oncoprotein-directed vaccine therapy has thus far been unsuccessful in patients with metastatic HPV^+ cancers (13–16).

The Immuno-STAT™ (Selective Targeting and Alteration of T cells) platform utilizes a highly modular molecular framework to directly modulate the activity of antigen-specific T cells *in vivo*. The novel mechanism of action of these fusion proteins harnesses two key signals for T-cell activation: T-cell receptor (TCR) engagement of a tumor-associated HLA-A*0201-peptide complex to induce activation, and delivery of affinity-attenuated IL2 to induce proliferation of tumor antigen-specific T cells. Together, the selective engagement and expansion of tumor antigen-specific T cells suggest potential for anticancer efficacy with reduced toxicity relative to nontargeted forms of immunotherapy that result in systemic activation of the immune system. As the first example in this molecular series, CUE-101 demonstrates selective binding, activation, and expansion of HPV16 $E7_{11-20}$-specific $CD8^+$ cytotoxic T cells, consistent with its design. This

[1]Cue Biopharma, Cambridge, Massachusetts. [2]BioKien LLC, Potomac, Maryland. [3]Departments of Biochemistry and Physiology and Biophysics, Albert Einstein College of Medicine, Bronx, New York. [4]The Brady Urological Institute, Johns Hopkins University School of Medicine, Baltimore, Maryland.

Note: Supplementary data for this article are available at Clinical Cancer Research Online (http://clincancerres.aacrjournals.org/).

Corresponding Authors: Mary Ellen Simcox, Cue Biopharma, 21 Erie St, Cambridge, MA 02139. Phone: 617-949-2605; E-mail: mesimcox@cuebio.com; and Steven Quayle, 617-949-2595; squayle@cuebio.com

Clin Cancer Res 2020;26:1953–64

doi: 10.1158/1078-0432.CCR-19-3354

Translational Relevance

Human papilloma virus (HPV)-associated head and neck squamous cell carcinoma (HNSCC) is emerging as a global epidemic. Despite recent approvals of immunotherapy drugs for the treatment of HNSCC and the limited clinical success that has been reported with therapeutic vaccines and CAR-T and adoptive cell therapies, metastatic disease remains largely incurable. The observation of objective clinical responses in early trials testing adoptive cell therapy with gene-engineered T cells targeting HPV16 E7 supports the concept that a single T-cell specificity can lead to antitumor activity in patients with HPV16-driven cancers. CUE-101 is a novel fusion protein that demonstrates selective binding, activation, and expansion of HPV16 $E7_{11-20}$-specific $CD8^+$ T cells in preclinical studies. *In vivo* studies confirm selective expansion of tumor-specific cytotoxic $CD8^+$ T cells, induction of immunologic memory, and a favorable safety profile, suggesting the potential for clinical efficacy in patients with $HPV16^+$ malignancies.

activity is observed *in vitro* in primary human cells and *in vivo* in HLA-A2 transgenic mice, and the therapeutic relevance of this mechanism is further supported by a murine surrogate (mCUE-101) that expands sufficient E7-specific $CD8^+$ T cells to promote antitumor efficacy and induce functional immunologic memory in the TC-1 tumor model. These data support the potential for CUE-101 to enhance antitumor immunity in HPV16-driven malignancies. CUE-101 is currently being evaluated in patients with $HPV16^+$ HNSCC (NCT03978689).

Materials and Methods

Manufacturing, purification, and characterization of Immuno-STAT proteins

Immuno-STAT proteins were expressed in CHO cells, either transiently in Expi-CHO cells (Thermo Fisher Scientific) or in stably producing lines. In general, proteins were purified from conditioned media using a two-step method of Protein A capture with MabSelect SuRe (GE) followed by size exclusion chromatography. Alternatively, the protein was purified using a three-step method, also employing MabSelect SuRe as a first step, followed by anion exchange chromatography and a hydroxyapatite polishing step.

Binding measurements were performed using bio-layer interferometry (Octet RED96e; ForteBio) with antihuman IgG Fc capture biosensor tips (Molecular Devices) to immobilize IL2Rα-Fc (Sino Biological) or IL2Rβ-Fc (Acro Biosystems). Interactions with anti-HLA (clone W6/32; Abcam) were measured by capturing CUE-101 and analogs on biosensor tips. Raw data were processed and analyzed with ForteBio's Data Analysis 11.0 software. For kinetic measurements, the processed curves were globally fit to a 1:1 binding model (17).

CTLL2 proliferation assay

CTLL2 cells (ATCC) were cultured in complete RPMI supplemented with IL2 (50 IU/mL). One day prior to testing, cells were washed with culture medium without IL2, resuspended at 1×10^5 cells/mL, and incubated for 24 hours at 37°C. Test article was then added, and after 3 days of treatment cell viability was assessed by measuring ATP levels via bioluminescence (CellTiter-Glo; Promega) according to manufacturer's instructions.

Cellular binding and phosphoflow analysis

E7 and CMV antigen-specific $CD8^+$ T cells (Astarte Biologics) were thawed, washed, and rested at 37°C. Cells were incubated with Immuno-STAT on ice for 5 minutes and binding was detected with an anti-human-IgG1 Fc-fluorescein isothiocyanate antibody (Abcam) for 15 minutes. For phosphoflow studies, cells were stimulated for 2 minutes (pSLP76) or 5 minutes (pSTAT5) at 37°C. Positive control stimulations included cross-linking anti-CD3/anti-CD28/anti-CD8 antibodies or recombinant human IL2. Cells were immediately fixed, permeabilized, and stained with anti-pY128 SLP76 or anti-pY694 STAT5 antibodies (BD Biosciences) for analysis on an Attune NxT flow cytometer (Invitrogen). The percent of positively stained cells was determined using FlowJo software (TreeStar).

ELISpots

Cells were thawed, washed, and resuspended in CTL-Test media (CTL) supplemented with 1% Glutamax (Gibco). E7 or CMV-specific cells were seeded at a density of 1,000 cells/well with media, Immuno-STAT, or PMA/ionomycin and incubated for 20 hours at 37°C in single enzymatic hu-IFNγ 96-well ELISpot plates (CTL). Plates were developed according to the manufacturer's instructions prior to signal quantitation (Immunospot S6 Universal Analyzer; CTL).

In vitro T-cell expansion

Human healthy donor peripheral blood mononuclear cells (PBMC) were obtained as frozen stocks (Astarte Biologics) or isolated from leukopaks (HemaCare). PBMCs were stimulated with CUE-101 in ImmunoCult-XF T Cell Expansion Media (Stemcell Technologies) for 10 days at 37°C with 50% media replacement every 2 to 3 days starting on day 5. As a control, PBMCs were stimulated for 10 days with 5 μg/mL of $E7_{11-20}$ peptide (Elim Biopharma) and IL2 (50 U/mL), with 50% media and IL2 replaced every 2 to 3 days starting on day 3. After 10 days, the cells were harvested and stained for downstream assays.

Tetramer staining and flow cytometry analysis

Prior to tetramer staining, murine cells were resuspended in 50 nmol/L dasatinib and incubated for 30 minutes at 37°C. Cells were washed, resuspended in Fixable Viability Stain 780 (BD Biosciences), and incubated for 15 minutes at 4°C. Cells were then pelleted and stained with tetramer (MBL International) diluted 1:20 in FACS buffer for 15 minutes at room temperature followed by surface staining for 20 minutes at 4°C. Fc receptor binding inhibitor (eBioscience) or 0.5 μg/mL mouse Fc Block (Clone 2.4G2; BD Biosciences) was also included. Cells were washed and fixed for 30 minutes at 4°C using the FoxP3 Fixation/Permeabilization Kit (eBioscience), washed, stained for FoxP3 for 30 minutes at room temperature, and analyzed on an Attune NxT cytometer.

Intracellular cytokine staining

A total of 2 to 4×10^6 human PBMCs expanded with CUE-101 or peptide were pretreated with Brefeldin A (BFA) and Monensin (Thermofisher), plated in a 24-well plate, and stimulated at a 1:1 ratio with T2 cells (ATCC) that had been loaded with 5 μg/mL of $E7_{11-20}$ (YMLDLQPETT) or HIV-1 p17 Gag_{77-85} (SLYNTVATL; SL9) peptide for 2 hours and washed twice. Alternatively, 2×10^6 murine cells were plated in a 96-well U-bottom plate and restimulated in CTL Test Medium containing 1% Glutamax by combining $E7_{49-57}$ peptide (RAHYNIVTF; 10 μg/mL) with BFA and Monensin diluted per the manufacturer's instructions. Expanded PBMCs or murine cells treated with media containing BFA and Monensin or Cell Stimulation Cocktail (Thermo Fisher Scientific) served as controls. Cells were stimulated

for 5 hours, washed, stained with FVS780 and surface markers as above, and fixed using IC fixation buffer (Thermo Fisher Scientific). Cells were next washed in permeabilization buffer (eBioscience), stained with intracellular antibodies for 30 minutes at room temperature, washed, and analyzed.

TCR sequencing and analysis of stable T-cell clones

PBMCs from healthy donors were expanded *in vitro* with $E7_{11\text{-}20}$ peptide plus IL2, or with 100 nmol/L CUE-101 in 10-day cultures. Expanded cells were harvested, tetramer stained, and $E7_{11\text{-}20}$-specific $CD8^+$ T cells were single cell sorted (Sony SH800) and the α and β TCR chains were coamplified (iRepertoire). TCR library sequencing used an Illumina MiSeq v2 Nano Kit. Data for each individual well were demultiplexed, mapped, and analyzed using the iRmap VDJ pipeline and the iPair Analyzer.

SKW-3 cells (DSMZ) were cultured in complete RPMI1640 without pen-strep. TCR lentiviral construct design followed the method of Jin and colleagues (18), and the generation of stable TCR-expressing SKW-3 cells is described in the Supplementary Materials and Methods. Assessment of CD69 upregulation was performed by loading T2 cells with peptide and coincubating with stable TCR transduced SKW-3 cells overnight at 37°C. The cells were stained for CD3, CD19, live/dead, and CD69 in the presence of Fc receptor inhibition, and analyzed.

Animals and tumor studies

All animal studies followed guidance from the SmartLabs Institutional Animal Care and Use Committee protocol MIL-100 and were performed in compliance with federal guidelines. Animal welfare was monitored daily and animal weights were collected twice a week. Early euthanasia criteria included >20% weight loss, body condition score ≤ 2, or tumor size of >20 mm on the longest side. Caliper measurements to calculate tumor volume ($L \times L \times W/2$) were collected three times per week. TC-1 cells were obtained from the laboratory of Dr. TC Wu (Johns Hopkins University) and were authenticated by IDEXX Cell Check Plus (not shown). For tumor studies, age-matched female albino C57Bl/6 (C57Bl/6-*Tyrp1*$^{b\text{-}J}$/J; Taconic) mice were implanted subcutaneously with 1.5×10^5 TC-1 cells suspended in PBS. For immunization studies, HLA-A2 (B6.Cg-Immp2l$^{Tg(HLA\text{-}A/H2\text{-}D)2Enge}$/J; Jackson Laboratories) mice were injected subcutaneously with $E7_{11\text{-}20}$ peptide, Tetanus Toxin Universal Helper Epitope $TT_{830\text{-}844}$ (QYIKANSKFIGITEL), and CpG ODN1826 (5′-tccatgacgttcctgacgtt-3′) diluted in 1× PBS. Preparation of tissue samples for analysis is described in Supplementary Materials and Methods.

Statistical analysis

Comparisons between two groups were performed by two-tailed Student *t* tests. For comparisons between multiple groups, one-way ANOVA followed by Tukey *post hoc* comparison was performed. *P* values ≤ 0.05 were considered significant. Comparisons of overall survival were conducted by log-rank test. All analyses were performed using GraphPad Prism (v8.0).

Results

Design and characterization of CUE-101

CUE-101 is composed of a single IgG1 Fc, two peptide–HLA complexes, and four reduced affinity human IL2 domains encoded in a two plasmid system (**Fig. 1A** and **B**). By presenting an immunodominant peptide epitope derived from the HPV16 E7 protein (amino acid residues 11-20: YMLDLQPETT), the CUE-101 molecule was designed to target HPV16 $E7_{11\text{-}20}$-specific $CD8^+$ T cells for the treatment of HLA-A*0201 patients with HPV16-positive malignancies. Two amino acid substitutions (L234A; L235A) were introduced in the Fc region of CUE-101 to reduce Fc domain effector function (19), allowing CUE-101 to maintain binding to FcRn while not exhibiting measurable binding to other Fc receptors or to C1q, except for FcRI (Supplementary Table 1; Supplementary Fig. S1A). Native conformation of the peptide-HLA component of CUE-101 was confirmed via binding of an anti-HLA class I mAb (Clone W6/32), which recognizes a conformational epitope encompassing the α3, α2, and β2-microglobulin domains (refs. 20, 21; Supplementary Fig. S1B). Analogs of CUE-101, namely CUE-1380-839 (containing CMV $pp65_{495\text{-}503}$ peptide) and CUE-1644-1274 (containing $E7_{11\text{-}20}$ peptide but lacking IL2 domains), showed similar binding to this antibody whereas the murine surrogate mCUE-101 (with murine IgG2a Fc and murine H-$2D^b$-$E7_{49\text{-}57}$ complexes) did not show significant binding (Supplementary Figs. S1C–S1E). Together, these data demonstrate effector attenuation of the Fc and confirm that the peptide–HLA component of CUE-101 is intact and properly folded.

To increase selectivity for target T cells and to minimize the potential for toxicity mediated through global IL2-driven activation of IL2 receptor (IL2R) expressing cells, two point mutations (H16A and F42A) were introduced into the IL2 sequences of CUE-101. Mutation of F42A was previously demonstrated to reduce IL2 interaction with the IL2Rα (IL2RA) chain (22), whereas H16A was hypothesized to reduce binding to the IL2Rβ (IL2RB) subunit based on structural analyses (23). As predicted, the binding affinity of a double mutant IL2 (H16A; F42A) for human IL2Rα and IL2Rβ was decreased 110- and 3-fold, respectively, compared with wild-type (WT) IL2 binding, predominantly due to a faster off-rate for each of these interactions (**Table 1**).

Functional attenuation of the mutant IL2 components of CUE-101 was shown in a CTLL-2 proliferation assay (**Fig. 1C**). Although CUE-101 stimulated proliferation of CTLL-2 cells, the potency of CUE-101 (EC_{50} = 26.56 nmol/L) was reduced ∼2,600-fold relative to recombinant human IL2, aldesleukin (EC_{50} = 0.01 nmol/L), confirming both the functionality of the mutant IL2 components of CUE-101 and their marked functional attenuation in an assay that is independent of TCR engagement. This finding supports the potential for CUE-101 to selectively activate antigen specific T cells in the absence of global stimulation of IL2R expressing cells.

CUE-101 selectively binds and activates $E7_{11\text{-}20}$-specific $CD8^+$ T cells through both the TCR and IL2R

Only HPV16 $E7_{11\text{-}20}$-specific $CD8^+$ T cells express both the TCR and IL2R necessary for full engagement of CUE-101, although immune cell lineages including $CD8^+$ and $CD4^+$ T cells, regulatory T cells, and NK cells could engage CUE-101 via the IL-2R. Selective binding of CUE-101 to HPV16 $E7_{11\text{-}20}$-specific $CD8^+$ T cells was demonstrated, whereas only minimal CUE-101 binding to CMV $pp65_{495\text{-}503}$-specific $CD8^+$ T cells, naïve $CD8^+$ T cells, and NK cells was observed (**Fig. 1D**; Supplementary Fig. S1F). CUE-101 binding induced phosphorylation of tyrosine 128 of the SH2 Domain-Containing Leukocyte Protein of 76 kDa (SLP76; LCP2) and phosphorylation of tyrosine 694 of the STAT5 protein, which serve as readouts for CUE-101 engagement of the TCR (24) and IL-2R (25), respectively. CUE-101 selectively induced SLP76 phosphorylation in HPV16 $E7_{11\text{-}20}$-specific $CD8^+$ T cells but not in bulk $CD8^+$ T cells from a healthy donor or in $pp65_{495\text{-}503}$-specific $CD8^+$ T cells (**Fig. 1E**). Likewise, CUE-101 induced potent and dose-dependent STAT5 phosphorylation in HPV16 $E7_{11\text{-}20}$-specific $CD8^+$ T cells (**Fig. 1F**).

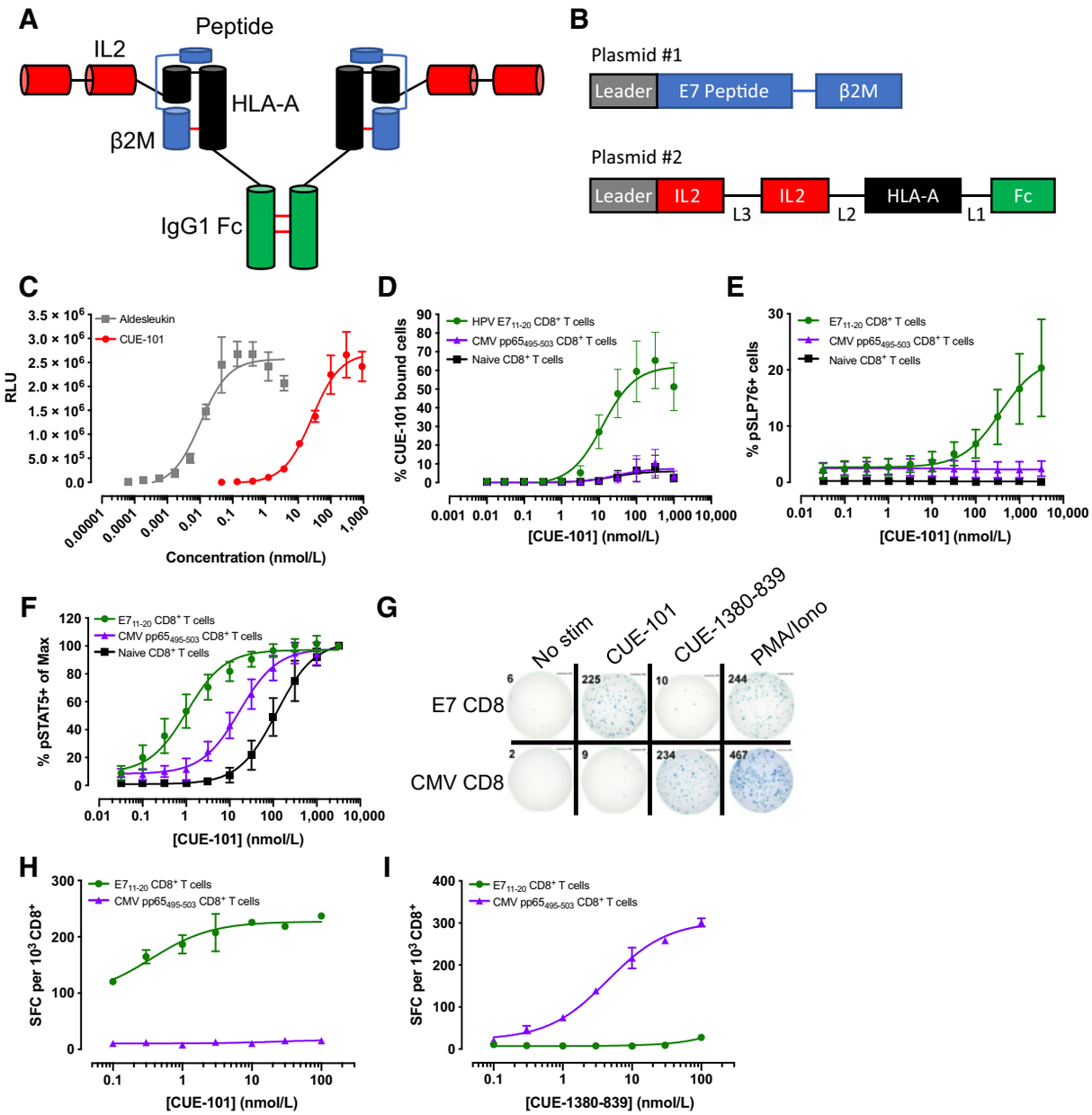

Figure 1.

CUE-101 selectively binds and activates antigen-specific CD8$^+$ T cells. **A,** Schematic representation of the design of CUE-101. **B,** Schematic representation of the two plasmids used to produce CUE-101. **C,** Relative light units (RLU) as a measure of CTLL-2 proliferation upon culture with CUE-101 or aldesleukin. Data shown are mean ± SD of nine technical replicates from a single experiment that is representative of two independent experiments. **D,** Percent of the indicated cell types that were bound by CUE-101 as assessed by flow cytometry. Data shown are mean ± SD from three independent experiments. **E,** Percent of the indicated cell types that stained positive for pSLP76 by flow cytometry. Data shown are mean ± SD from three independent experiments. **F,** Percent of the indicated cell types that stained positive for pSTAT5 by flow cytometry. Data shown are mean % of max ± SD from three independent experiments. **G,** Representative images of IFNγ ELISpot wells upon stimulation of E7 or CMV-specific T cells with the indicated agents. **H** and **I,** Frequency of IFNγ positive spots upon stimulation of E7 or CMV-specific T cells with CUE-101 or CUE-1380-839. Data shown are mean ± SD from a representative experiment repeated at least three times.

Together these results support that the peptide-HLA moiety of CUE-101 directs the selective binding and activation of TCR and IL2R signaling events in antigen-specific T cells.

In addition to cellular binding and the observed signaling events, CUE-101 also induced potent and dose-dependent secretion of IFNγ (IFNG), a T-cell effector cytokine, from primary purified human $E7_{11-20}$-specific T cells (**Fig. 1G** and **H**). Removal of the IL2 domains in CUE-1644-1274 significantly reduced the potency of effector cell stimulation (Supplementary Fig. S1G). In contrast, CUE-101 treatment did not activate CMV $pp65_{495-503}$-specific T cells (**Fig. 1G** and **H**). Through substitution with the $pp65_{495-503}$ peptide,

Table 1. Double H16A; F42A mutation of IL2 reduced binding affinity to human IL2Rα and β subunits.

Construct	Human IL2R	$K_D \pm$ SD (nmol/L)	$k_{on} \pm$ SD (M^{-1} s^{-1})	$k_{off} \pm$ SD (s^{-1})
WT IL2-FLAG	IL2Rα	10.7 ± 1.4	$5.5 \times 10^5 \pm 1.6 \times 10^5$	$5.8 \times 10^{-3} \pm 1.5 \times 10^{-3}$
H16A; F42A IL2-FLAG	IL2Rα	1180 ± 124.9	$3.1 \times 10^5 \pm 2.3 \times 10^5$	$5.2 \times 10^{-1} \pm 0.4 \times 10^{-1}$
WT IL2-FLAG	IL2Rβ	197.0 ± 1.6	$5.9 \times 10^5 \pm 1.2 \times 10^5$	$1.2 \times 10^{-1} \pm 0.2 \times 10^{-1}$
H16A; F42A IL2-FLAG	IL2Rβ	613.2 ± 31.0	$7.1 \times 10^5 \pm 2.0 \times 10^5$	$4.4 \times 10^{-1} \pm 1.3 \times 10^{-1}$

a CMV-specific Immuno-STAT (CUE-1380-839) was generated that specifically activated $pp65_{495\text{-}503}$-specific T cells but not $E7_{11\text{-}20}$-specific T cells (**Fig. 1G** and **I**). These findings demonstrate that the peptide-HLA moiety of Immuno-STAT molecules guides selective activation of antigen-specific T cells.

CUE-101 selectively expands polyfunctional $E7_{11\text{-}20}$-specific $CD8^+$ T cells from human PBMCs

To demonstrate that CUE-101 can enhance antitumor immunity through the selective expansion of $E7_{11\text{-}20}$-specific T cells, PBMCs from a healthy HLA-A*0201-positive donor were stimulated with CUE-101, incubated for 10 days, and analyzed by flow cytometry after staining with HLA-A*0201 tetramers presenting the HPV16 $E7_{11\text{-}20}$ peptide (**Fig. 2A**; Supplementary Fig. S2A). Treatment with CUE-101 alone induced a concentration-dependent and selective expansion of $E7_{11\text{-}20}$-specific $CD8^+$ T cells from undetectable frequencies at baseline, with maximal expansion observed upon stimulation with 100 nmol/L CUE-101 (**Fig. 2B**). Similar expansion was observed in PBMCs from a second donor (Supplementary Fig. S2B). CUE-101 also induced expansion of NK cells with minimal or no expansion of $CD4^+$ T cells, total $CD8^+$ T cells, or regulatory T cells (**Fig. 2B**).

Functionality of the CUE-101 expanded $E7_{11\text{-}20}$-specific $CD8^+$ T cells was demonstrated by measuring production of effector cytokines and markers of degranulation in response to stimulation by peptide-pulsed T2 cells (Supplementary Fig. S2C). The CUE-101 expanded tetramer positive T cells stimulated with $E7_{11\text{-}20}$-loaded cells demonstrated strong induction of IFNγ, TNFα (TNF), and CD107a (LAMP1; **Fig. 2C**). These markers were not induced upon stimulation with irrelevant HIV $Gag_{77\text{-}85}$ (SL9)-loaded cells, nor in non-antigen–specific $CD8^+$ T cells stimulated with either peptide (**Fig. 2D** and **E**). These results confirm the antigen specificity of the CUE-101 expanded T cells and provide evidence of multiple CTL-like effector functions in response to target cells. TCR repertoire diversity was examined by single-cell TCRα-chain and TCRβ-chain sequencing of tetramer$^+$ $CD8^+$ T cells that were expanded from PBMCs of two healthy donors via CUE-101 or peptide/IL2 stimulation. Although the $CD8^+$ T cells expanded from one donor represented a single TCR specificity, the second donor displayed multiple unique TCR clones, demonstrating that CUE-101, like native peptide, is able to stimulate a polyclonal population of TCRs specific for the HPV16 $E7_{11\text{-}20}$ peptide (**Fig. 2F**). Finally, the two dominant TCRs identified in this analysis were constitutively expressed in SKW-3 cells and were shown to be responsive to both $E7_{11\text{-}20}$ and $E7_{11\text{-}19}$ peptide stimulation (**Fig. 2G**), demonstrating that CUE-101 expands effector $CD8^+$ T cells capable of responding to both of these immunodominant peptide epitopes (10, 11).

CUE-101 treatment expands $E7_{11\text{-}20}$-specific $CD8^+$ T cells in naïve and immunized mice

The *in vivo* activity of CUE-101 was tested in HLA-A2 transgenic mice that express a chimeric HLA class I molecule composed of the α1 and α2 domains from human HLA-A2.1 and the α3 transmembrane/cytoplasmic domain from murine $H\text{-}2D^d$ (26). Weekly intravenous treatment of immunologically naïve HLA-A2 mice with CUE-101 elicited a population of $E7_{11\text{-}20}$-specific $CD8^+$ T cells in the blood and spleen that was not observed with vehicle treatment (**Fig. 3A** and **B**; Supplementary Fig. S3). No significant changes in the frequencies of $CD4^+$, $CD8^+$, Treg, NKT, or NK nontarget cells were observed in the peripheral blood or spleen, demonstrating antigen-specific cellular targeting with CUE-101 *in vivo* (**Fig. 3C**). CUE-101 was well tolerated with no observations of treatment-related clinical signs or body weight loss. Effector T-cell activation, as characterized by antigen-specific IFNγ production following *ex vivo* peptide stimulation, confirmed that the antigen-specific T cells expanded through *in vivo* treatment possess CTL-like properties (**Fig. 3D** and **E**).

The ability of CUE-101 to expand an existing population of antigen-specific $CD8^+$ memory T cells was assessed in HLA-A2 transgenic mice that were first immunized with $E7_{11\text{-}20}$ peptide to generate a specific $CD8^+$ T-cell population and then randomized on the basis of the frequency of $E7_{11\text{-}20}$-specific $CD8^+$ T cells. Mice were rested for 3 weeks after the final boost (baseline; **Fig. 3F**) and then treated with vehicle or CUE-101. As in the naïve setting, intravenous treatment with CUE-101 resulted in expansion of the $E7_{11\text{-}20}$-specific $CD8^+$ T-cell population in blood relative to the baseline frequency prior to treatment, whereas vehicle treatment did not result in E7-specific T-cell expansion (**Fig. 3G**). The functionality of the expanded $CD8^+$ T cells was demonstrated via detection of antigen-specific IFNγ production following *ex vivo* peptide stimulation (**Fig. 3H**). Thus, intravenous treatment with CUE-101 alone was sufficient to expand an $E7_{11\text{-}20}$-specific population from both a naïve $CD8^+$ T-cell repertoire and an existing T-cell population.

Treatment with a murine surrogate of CUE-101 expands polyfunctional $E7_{49\text{-}57}$-specific $CD8^+$ T cells in the tumor, spleen, and blood of TC-1 tumor-bearing mice

A murine surrogate of CUE-101 (mCUE-101) with functionally equivalent domains was generated to assess activity in immunocompetent tumor-bearing mice. mCUE-101 retains the design of CUE-101, with an effector attenuated murine IgG2a Fc, an $H\text{-}2D^b\text{-}E7_{49\text{-}57}$ peptide–MHC complex, and identical human mutant IL2 components. Human IL2 is cross-reactive with mouse IL2R, modeling human IL2 effects on mouse cells and in mouse tumor models (27). As T-cell activation induces upregulation of PD-1 (PDCD1), and PD-1–blocking antibodies are approved for the treatment of patients with HNSCC, combination therapy with mCUE-101 and anti-PD-1 checkpoint blockade was also explored.

The TC-1 murine tumor model expresses the HPV16 E6 and E7 oncoproteins, and HPV16 E7 vaccination strategies were previously shown to mediate antitumor efficacy in this model (28) whereas single-agent anti-PD-1 treatment did not (29, 30). The antitumor activity of mCUE-101 was assessed in immunocompetent C57BL/6 mice with treatment initiation after TC-1 tumors were established. Significant

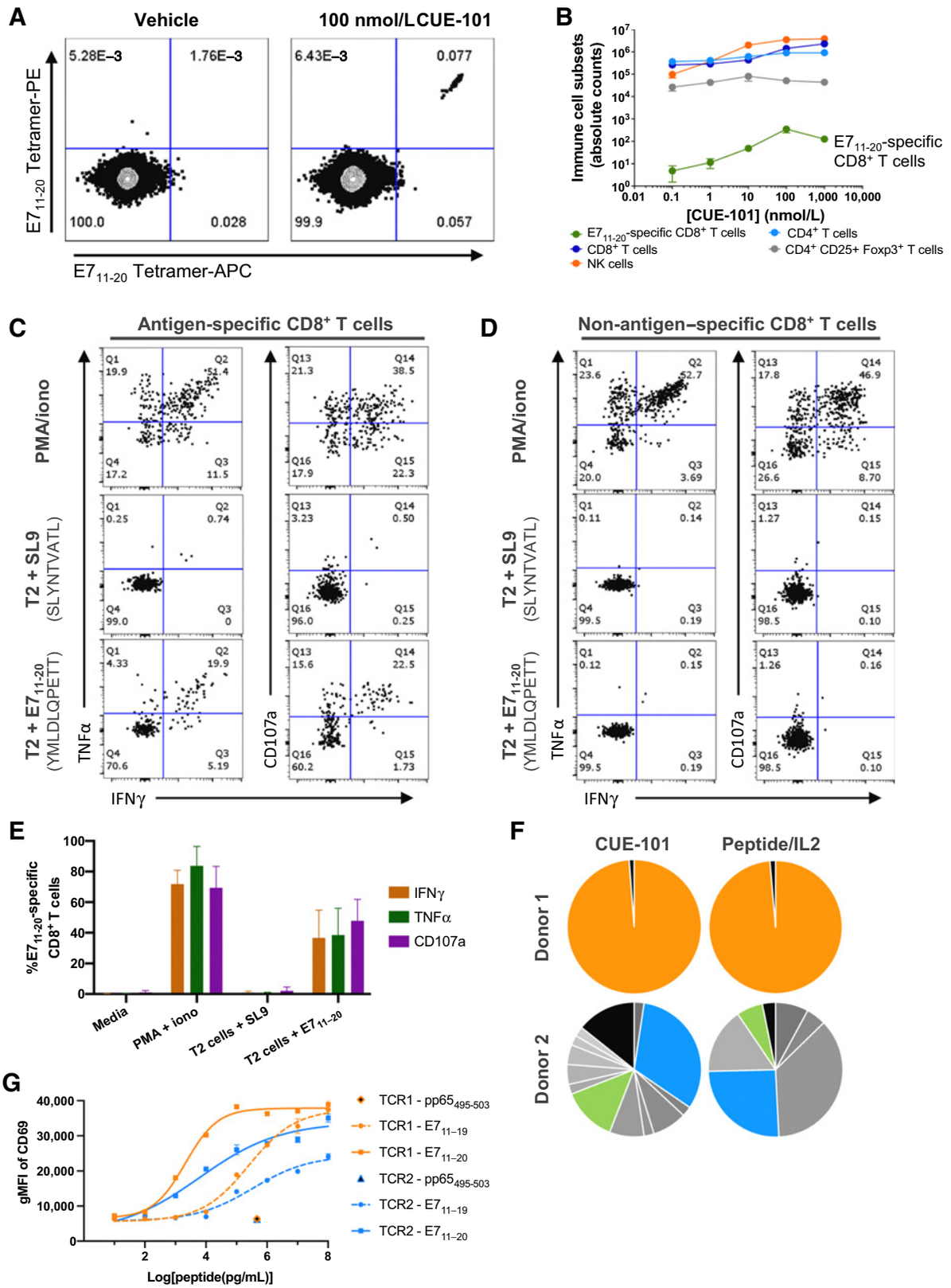

tumor growth inhibition and prolongation of survival were observed after mCUE-101 administration, but no animals demonstrated complete tumor regression (**Fig. 4A**; Supplementary Fig. S4A). To assess the pharmacodynamic effects of treatment in this setting, tumors, spleens, and peripheral blood were harvested 6 days after the final treatment with mCUE-101 at a time when tumor growth inhibition was observed. Single-agent mCUE-101 was well tolerated, with only small, but significant, reductions in NK cells in the blood and $CD4^+$ T cells in the spleen (Supplementary Fig. S4B). In the tumors, though, combination treatment was associated with a significant increase in the frequency of total $CD8^+$ and $CD4^+$ T cells as well as NK cells, suggesting enhanced tumor immune infiltration (Supplementary Fig. S4B). Furthermore, the frequency of $E7_{49\text{-}57}$-specific T cells among all tumor-infiltrating $CD8^+$ T cells was significantly increased by single-agent mCUE-101 treatment ($P < 0.001$), and further enhanced by combination treatment, where on average >50% of the $CD8^+$ tumor infiltrate was antigen-specific and there was also a significant increase in the CD8:Treg ratio ($P < 0.001$; **Fig. 4B–D**). E7-specific $CD8^+$ T cells were not expanded in tumors from mice treated with anti-PD-1 alone. In the spleens and peripheral blood of mCUE-101–treated animals, there was also a trend toward increased frequencies of E7-specific $CD8^+$ T cells, which was significantly increased upon combination treatment ($P < 0.01$; **Fig. 4E**; Supplementary Fig. S4C). Responsiveness of the expanded T cells to cognate peptide presentation was assessed via intracellular cytokine staining of whole tumor-infiltrating lymphocyte (TIL) and splenocyte populations from treated animals that were stimulated *ex vivo* with $E7_{49\text{-}57}$ peptide. Among tumor-infiltrating $CD8^+$ T cells, and consistent with the tetramer staining results, single-agent mCUE-101 treatment resulted in a significant increase in the frequency of cells that were positive for IFNγ and double positive for CD107a and Granzyme B (Gzmb) in response to peptide challenge ($P < 0.01$), and these frequencies were further increased upon combination treatment ($P < 0.05$; **Fig. 4F**). Similarly, increased frequencies of polyfunctional E7-specific $CD8^+$ T cells were also observed in splenocytes (**Fig. 4G**), confirming that the E7-specific $CD8^+$ cells expanded by mCUE-101 treatment were able to function as cytotoxic T lymphocytes and promote enhanced antitumor immunity. Significant upregulation of PD-1 surface expression on E7-specific T cells in mCUE-101–treated animals was observed when compared to the non-antigen–specific $CD8^+$ T cells in the blood and spleen, and the magnitude of this effect was even greater within the tumor ($P < 0.001$; **Fig. 4H**), providing further confirmation of in situ activation of the tumor antigen-specific T cells expanded by mCUE-101 treatment.

Treatment with mCUE-101 promotes antitumor immunity and functional immunologic memory

The antitumor activity of mCUE-101 was further assessed by initiating treatment 24 hours after subcutaneous implantation of TC-1 tumor cells. Treatment with mCUE-101 significantly increased survival in this model ($P = 0.005$), expanded a population of E7-specific $CD8^+$ T cells in the periphery, and resulted in 10% (1/10) of animals being tumor-free 79 days post-implantation (**Fig. 5A** and **B**; Supplementary Fig. S5A). This antitumor activity is specific to mCUE-101 as an analog targeting a different peptide specificity (LCMV $GP33_{33\text{-}41}$; CUE-1843-835) did not inhibit tumor growth or expand $E7_{49\text{-}57}$-specific $CD8^+$ T cells in this model, though it did expand a population of $GP33_{33\text{-}41}$-specific $CD8^+$ T cells (Supplementary Fig. S5B and S5C).

Combination treatment with mCUE-101 and anti-PD-1 further increased survival ($P = 0.003$), E7-specific $CD8^+$ T-cell frequency ($P < 0.05$), and antitumor activity relative to mCUE-101 monotherapy, including an increase in the number of animals remaining tumor-free (60%; 6/10) up to 79 days postimplantation (**Fig. 5A** and **B**; Supplementary Fig. S5A). All treatments were well tolerated without clinical signs or body weight loss. Comparable increases in the frequency of E7-specific $CD8^+$ T cells were observed in the tumors, spleens, tumor-draining lymph nodes, and peripheral blood of animals in the setting of treatment soon after tumor implantation (Supplementary Fig. S6A). Significant upregulation of PD-1 on tumor-infiltrating E7-specific $CD8^+$ T cells was also observed upon treatment in this setting ($P < 0.01$; Supplementary Figs. S6B and S6C). This upregulation of PD-1 expression provides a mechanistic rationale underlying the significantly enhanced antitumor efficacy observed upon combination treatment with anti-PD-1 blockade, and demonstrates a consistency of effect in both early and established treatment settings that suggests the greater tumor control in the early treatment setting may be due to the earlier expansion of the relevant T-cell population prior to the rapid outgrowth of the tumor.

Induction of immunologic memory was assessed in mice that remained tumor-free 95 days after initial challenge and combination therapy by rechallenging animals with TC-1 tumors. Upon implantation all treatment naïve animals formed tumors, whereas animals previously treated with combination therapy rapidly rejected the tumors, demonstrating immunologic memory was established with mCUE-101 treatment (**Fig. 5C**). Depletion of $CD8^+$ T cells in tumor-free mice prior to rechallenge resulted in tumor formation similar to that observed in tumor naïve mice, supporting the mechanism of action of mCUE-101 (**Fig. 5D**). In contrast, depletion of $CD4^+$ T cells or treatment with an anti-IgG2b isotype control antibody was associated with significantly longer survival, suggesting that $CD4^+$ T cells are not required for protective immunologic memory in this model. Together, these results demonstrate that a murine surrogate of CUE-101 is able to activate specific antitumor immunity, expand a therapeutically relevant frequency of E7-specific $CD8^+$ T cells, and induce functional immunologic memory, which is significantly enhanced in the setting of combination therapy with anti-PD-1 blockade. These results support the potential for CUE-101 to elicit and expand E7-specific $CD8^+$ T cells to stimulate antitumor immunity in patients with HPV16-driven tumors, and provide a rationale to further test combination therapy with immune checkpoint blockade in these patients.

Figure 2.

CUE-101 expands polyfunctional $E7_{11\text{-}20}$-specific $CD8^+$ T cells from human PBMCs. **A,** Representative dot plot demonstrating a double tetramer positive population of E7-specific T cells after CUE-101 treatment. **B,** Absolute numbers of the indicated cell types in human PBMCs after stimulation with increasing concentrations of CUE-101. Data shown are mean ± SEM from a single experiment. **C** and **D,** Representative dot plots demonstrating that $CD8^+$ T cells that bind $E7_{11\text{-}20}$-HLA-A*0201 tetramer produce IFNγ, TNFα, and CD107a in response to stimulation with $E7_{11\text{-}20}$ peptide whereas tetramer negative $CD8^+$ T cells do not. **E,** Percent of $E7_{11\text{-}20}$-specific $CD8^+$ T cells upregulating IFNγ, TNFα, or CD107a in response to the indicated stimulus. Data shown are mean ± SD from two independent experiments. **F,** Pie charts showing the relative proportion of individual TCR sequences amongst all those sequenced post CUE-101 treatment. Each color represents a single TCR clone, with identical colors identifying those sequences that are shared between samples. Shades of gray indicate unique TCR clones; black is all TCRs that were only identified once. **G,** Geometric median fluorescence intensity (gMFI) of CD69 expression on SKW-3 cells expressing the two most dominant TCRs identified in **F**. Cells were stimulated by T2 cells loaded with $E7_{11\text{-}20}$ or $E7_{11\text{-}19}$ peptide. Data shown are mean ± SD from duplicate wells and are representative of three independent experiments.

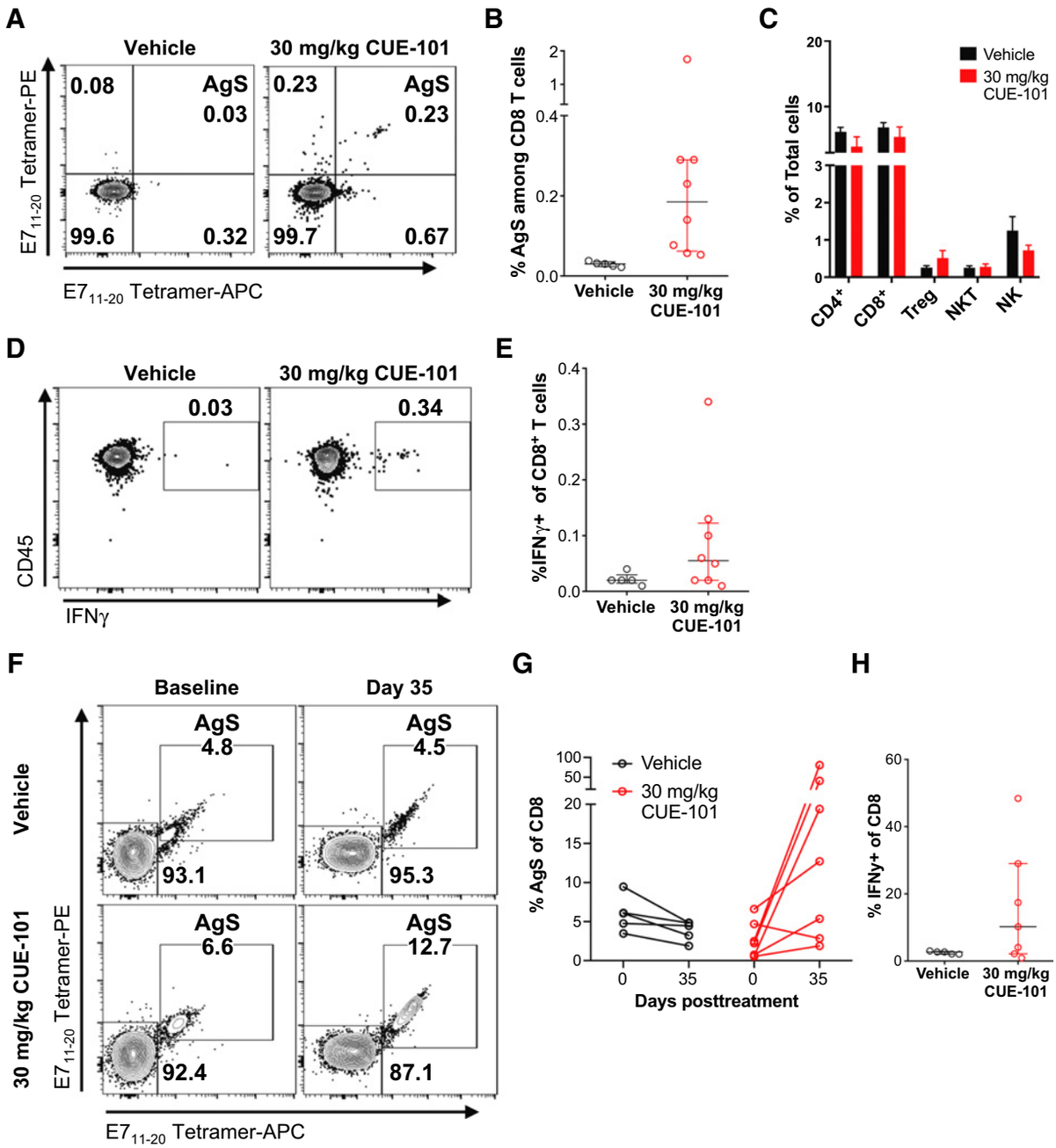

Figure 3.

CUE-101 selectively expands $E7_{11-20}$-specific $CD8^+$ T cells in HLA-A2 transgenic mice. **A,** Weekly intravenous dosing of CUE-101 over 29 days induced $E7_{11-20}$-specific $CD8^+$ T-cell expansion in blood as demonstrated by flow cytometry after staining with differentially labeled HLA-A*0201:$E7_{11-20}$ tetramers. Blood was sampled 6 days following the last dose. **B,** Frequencies of $E7_{11-20}$-specific $CD8^+$ T cells in the blood of HLA-A2 mice receiving the indicated treatment ($n = 8–9$; data shown indicate median ± interquartile range). **C,** Immunophenotyping by flow cytometry shows that repeat CUE-101 dosing did not impact nontarget immune cell frequencies in blood relative to vehicle treated animals ($n = 8–9$; data shown indicates mean ± SD). **D,** Representative plots of frequency of $CD8^+$ $CD45^+$ IFNγ producing cells after *ex vivo* $E7_{11-20}$ peptide stimulation. **E,** CUE-101 treatment increased the frequency of IFNγ -producing $CD8^+$ T cells as measured by flow cytometry ($n = 8–9$; data shown indicate median ± interquartile range). **F,** Representative flow plots demonstrating that CUE-101 treatment expanded $E7_{11-20}$-specific $CD8^+$ T cells in the blood of peptide immunized HLA-A2 mice. Mice were vaccinated three times, 9 to 11 days apart, and blood was sampled 6 days following the last CUE-101 dose. **G,** Frequencies of $E7_{11-20}$-specific $CD8^+$ T cells in the blood of immunized HLA-A2 mice at baseline, prior to treatment, and after receiving the indicated treatment ($n = 5–7$). **H,** CUE-101 treatment increased the frequency of IFNγ -producing $CD8^+$ T cells as measured by flow cytometry ($n = 5–6$; data shown indicate median ± interquartile range).

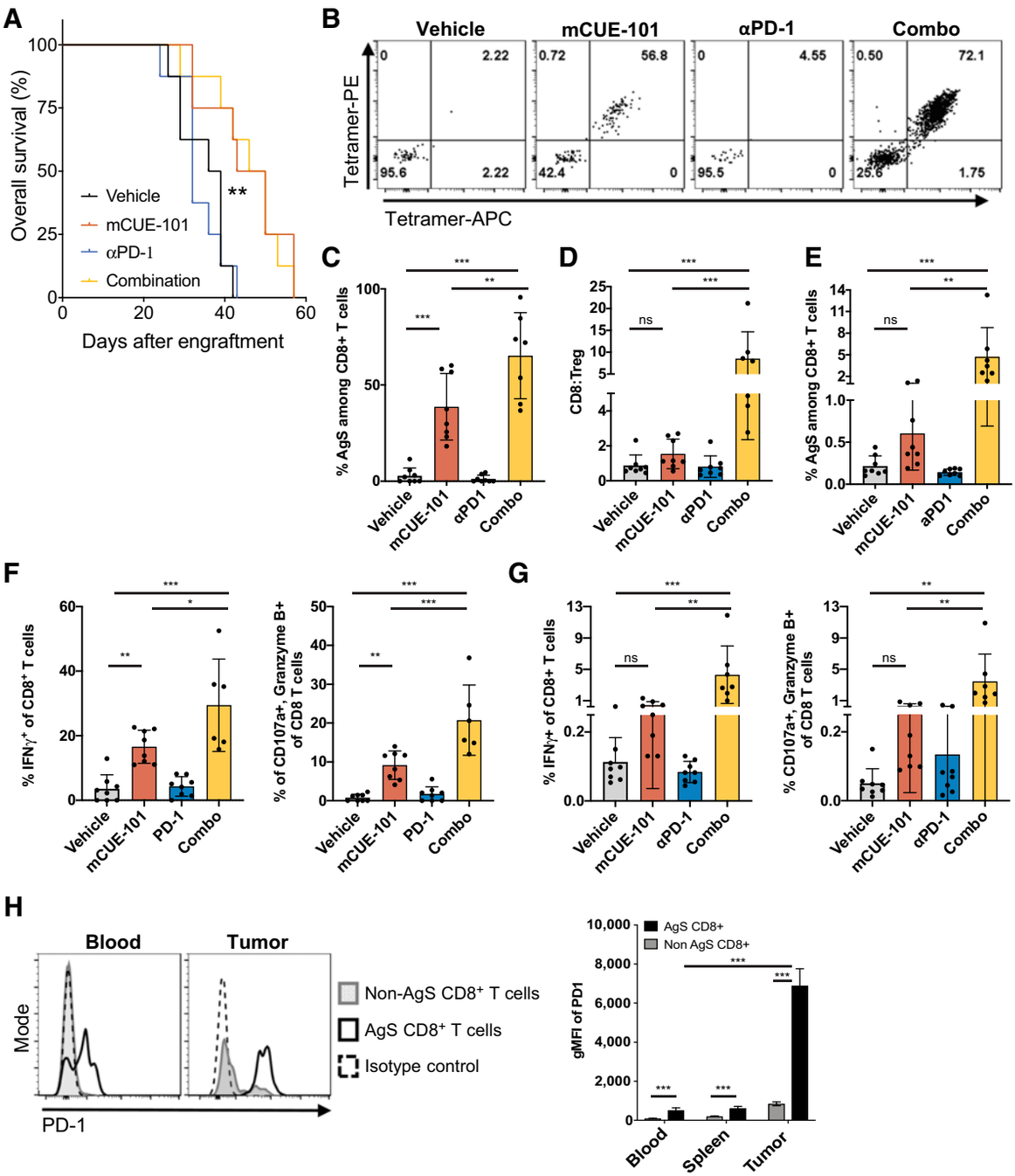

Figure 4.

A murine CUE-101 surrogate, mCUE-101, increases the frequency of polyfunctional E7-specific CD8$^+$ T cells infiltrating TC-1 tumors. **A,** Kaplan–Meier plot of overall survival of mice bearing staged TC-1 tumors after treatment with the indicated agents ($n = 8$ per group). Mice were randomized into groups with mean tumor volumes of ~50 mm^3/group on Day 9 of the study and dosing was initiated. mCUE-101 was administered subcutaneously twice daily for the first 2 days of a weekly regimen, and repeated for 2 weeks (i.e., twice daily on Days 9, 10, 16, and 17 postimplantation). Anti-PD-1 was administered via the intraperitoneal route three times per week for 2 weeks. $^{**}P < 0.01$ by log-rank test between vehicle and either single-agent mCUE-101 or combination treatment. **B,** Representative dot plots of double tetramer positive CD8$^+$ T cells within the tumor. **C,** Frequency (mean ± SD) of antigen-specific (AgS) T cells within the tumors of the indicated treatment groups. **D,** CD8:Treg ratio (mean ± SD) among tumor-infiltrating CD3$^+$ T cells. **E,** Frequency of AgS cells among CD8$^+$ T cells in the spleen. **F,** Frequency of CD8$^+$ T cells in the tumor (mean ± SD) producing the indicated proteins in response to peptide stimulation. **G,** Frequency of CD8$^+$ T cells in the spleen (mean ± SD) producing the indicated proteins in response to peptide stimulation. **H,** Representative histogram of PD-1 expression level on the surface of E7-specific CD8$^+$ T cells from mice treated with single agent mCUE-101. Graph shows gMFI of PD-1 expression (mean ± SD) of E7-specific (black) vs. nonspecific (gray) CD8$^+$ T cells in the indicated tissues. *, $P < 0.05$; **, $P < 0.01$; ***, $P < 0.001$; ns, not significant by one-way ANOVA with Tukey *post hoc* comparison.

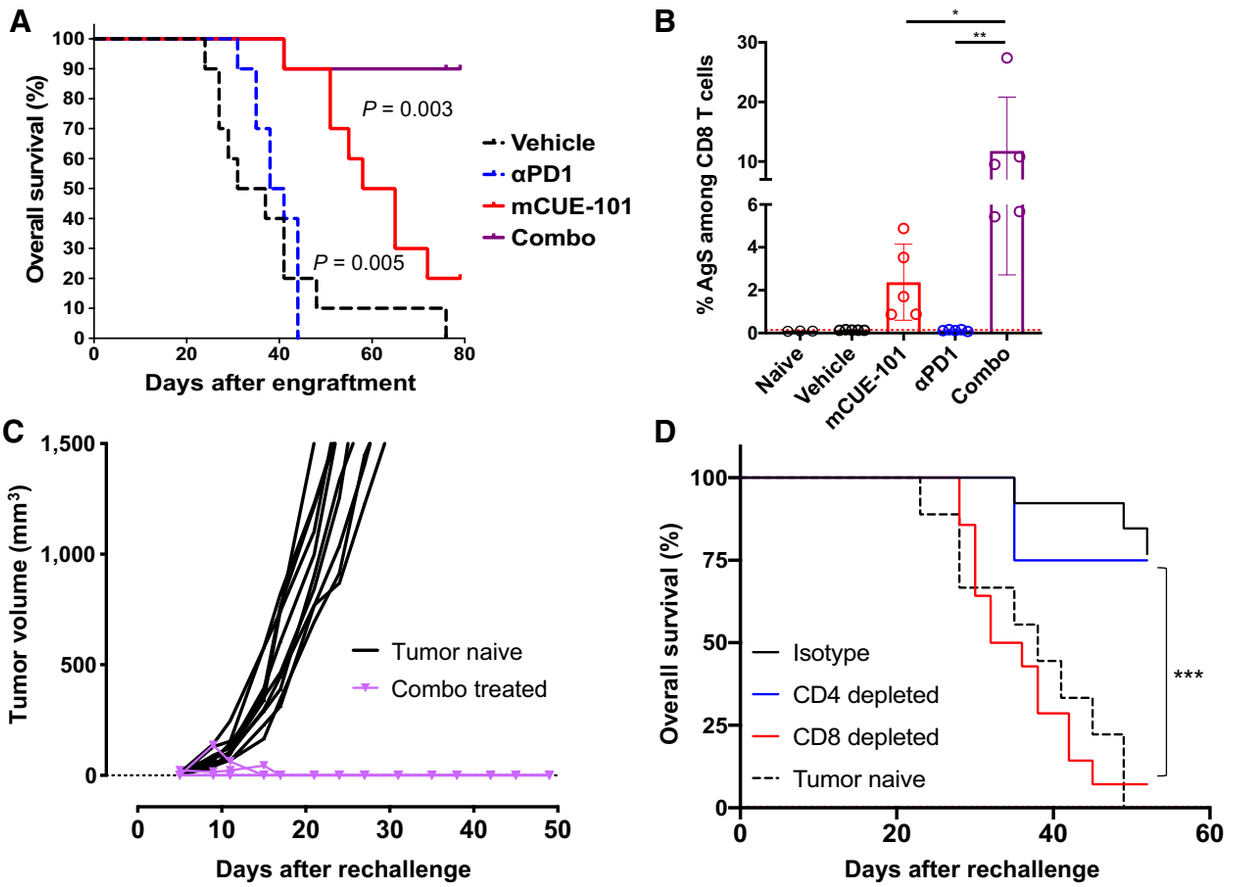

Figure 5.

Murine CUE-101 increases survival and induces immunologic memory in mice. **A,** Kaplan–Meier plot of overall survival after treatment with the indicated agents ($n = 10$ per group). Dosing was initiated 24 hours post engraftment, prior to development of palpable tumors. mCUE-101 was administered subcutaneously twice daily for the first 2 days of a weekly regimen, and repeated for 2 weeks (i.e., twice daily on Days 1, 2, 8, and 9 postimplantation). Anti-PD-1 was administered via the intraperitoneal route three times per week for 2 weeks. Statistical significance was assessed by log-rank test between vehicle and single-agent mCUE-101, and between mCUE-101 and combination treatment. **B,** Frequency of $E7_{11\text{-}20}$ antigen-specific (AgS) $CD8^+$ T cells in the peripheral blood of animals on Day 16 posttumor engraftment ($n = 5$; data shown are mean ± SD). $^*P < 0.05$, $^{**}P < 0.01$ by one-way ANOVA with Tukey *post hoc* comparison. **C,** Mice that remained tumor free after initial mCUE-101 plus anti-PD-1 combination treatment ($n = 5$) rejected TC-1 tumors upon rechallenge in the absence of additional treatment. **D,** Mice that remained tumor-free after initial therapy were depleted of T-cell lineages through administration of anti-CD8, anti-CD4, or isotype control antibodies prior to rechallenge. Mice that were depleted of $CD8^+$ T cells formed tumors similarly to tumor naïve mice ($n = 4$–14; data are Kaplan–Meier survival curves combined from two independent studies). ***, $P < 0.001$ by log-rank test.

Discussion

This report describes the application of the Immuno-STAT platform to the development of a novel therapeutic candidate, CUE-101. In model systems, CUE-101 demonstrates selective activation and expansion of antigen-specific $CD8^+$ T cells that mediate tumor clearance and establish antitumor immunologic memory. These preclinical data and the novel mechanism of action support the use of CUE-101 to address multiple HPV16-driven malignancies. CUE-101 is currently being tested as a monotherapy in $HPV16^+$ patients with HNSCC (NCT03978689).

Clinical relevance of tumor-specific T cells for cancer immunotherapy is demonstrated by objective clinical responses after adoptive transfer of autologous TILs, including when only a few tumor-targeting T-cell specificities were represented in the TIL population (31, 32), or when T cells were engineered to express a single TCR (33). However, these therapies require extensive and specialized *ex vivo* manipulation of patient-derived cells and challenging preconditioning regimens to promote survival of the transferred cells. Recombinant IL2 (aldesleukin) therapy also enhances antitumor immunity (34), but toxicities associated with aldesleukin curbs its use in the clinic and expansion of Tregs may limit its effectiveness (35, 36). Vaccination approaches can have similar limitations, where long peptides have generated both effector and Treg responses (37). In contrast, CUE-101 is a single molecule with the minimal essential signals for direct activation of antigen-specific $CD8^+$ T cells, functioning as an off-the-shelf therapeutic to enhance antigen-specific T-cell responses without requiring *ex vivo* manipulation. Functional attenuation of the IL2 components of CUE-101 reduces the potential for aldesleukin-associated toxicities, and for activation of other IL2R expressing cell types that may limit its activity. As a result, CUE-101 exposure leads to selective expansion of $E7_{11\text{-}20}$-specific $CD8^+$ T cells without significant expansion of Tregs *in vitro* and *in vivo*, and its peptide-HLA specificity precludes the generation of an antigen-specific Treg response that could limit therapeutic potential.

CUE-101 targets a single peptide specificity, yet treatment of human PBMCs demonstrates that CUE-101 can activate and expand a polyclonal $CD8^+$ T-cell repertoire, including multiple unique TCRs capable of recognizing and responding to the $E7_{11\text{-}20}$ peptide. Thus, in this molecular framework a single peptide–HLA complex does not limit response to a single TCR. Although $E7_{11\text{-}20}$ has been identified as an immunodominant HLA-A*0201 epitope (10), the $E7_{11\text{-}19}$ peptide is also naturally processed and presented on cancer cells (11). Thus, it is significant that the two TCRs identified and tested from CUE-101 expanded $CD8^+$ T cells were able to recognize both the $E7_{11\text{-}20}$ and $E7_{11\text{-}19}$ peptides, suggesting that if only one of these peptides is processed and presented in a given patient CUE-101 will expand a relevant CTL population. Therefore, CUE-101 has the potential to harness a diverse, native T-cell repertoire to mount an effective antitumor immune response while avoiding systemic activation of the immune system.

The activity of a murine surrogate in the immunocompetent TC-1 tumor model provides a mechanistic rationale for combination activity of CUE-101 with PD-1 checkpoint blockade in the clinic. Activation of T cells leads to upregulation of PD-1 expression (38), which is consistent with the observed PD-1 upregulation on the surface of E7-specific $CD8^+$ T cells after treatment with mCUE-101. CUE-101 treatment may thus lead to significant expansion of $E7_{11\text{-}20}$-specific $CD8^+$ T cells in patients, but activation-induced expression of PD-1 may limit their ability to kill E7 expressing tumor cells. Preclinical data presented here support that CUE-101 in combination with a PD-1 blocking antibody may overcome this mechanism that might limit clinical activity. A recent clinical trial testing PD-1 blockade in combination with an E6/E7 vaccination approach resulted in a favorable clinical response rate (39), further supporting this combination approach with CUE-101. The therapeutic benefit of CUE-101 plus PD-1 blockade was not as strong in the late treatment setting despite achieving the desired pharmacodynamic effect *in vivo*, suggesting additional immune stimulation may be needed to treat advanced disease or to overcome an immunosuppressive tumor microenvironment. Further characterization of the tumor microenvironment and understanding mechanisms of escape in the TC-1 model may provide clinically relevant information for the development of CUE-101. For example, much work is ongoing in the field to develop agents specifically designed to overcome mechanisms of escape, which may represent opportunities to enhance antitumor immunity in combination with CUE-101. In addition, deep phenotypic characterization of the $E7_{11\text{-}20}$-specific $CD8^+$ T cells expanded by CUE-101 preclinically and in patients may reveal additional rational combination approaches for future testing to overcome these potential limitations.

Although CUE-101 specifically targets $E7_{11\text{-}20}$ specific T cells, there is also potential for this class of molecules to have activity across different cancer indications. In support of this, the CMV- and LCMV-targeted analogs used in this study were also able to selectively activate and expand their respective T-cell specificities. Additional analogs targeting tumor-associated antigens represent potential candidates for development of molecules for other cancer indications. Ongoing and future research may also identify features of the tumor microenvironment where the optimal biological effect would be provided by an immunomodulatory signal other than IL2. The unique modular nature of this class of molecules thus provides flexibility with potential for broad applicability in the development of additional novel cancer treatments.

Disclosure of Potential Conflicts of Interest

S.N. Quayle, D.R. Thapa, Z. Merazga, M.M. Kemp, A. Histed, F. Zhao, M. Moreta, P. Ruthardt, L. Witt, J. Ryabin, J.F. Ross, P.A. Kiener, R. Chaparro, R. Seidel, A. Suri, S. Cemerski, K.J. Pienta, and M.E. Simcox are employees/paid consultants for and hold ownership interest (including patents) in Cue Biopharma. N. Girgis holds ownership interest (including patents) in Cue Biopharma. D.R. Beal, J. Soriano, M. Haydock, and E. Spaulding are employees/paid consultants for Cue Biopharma. S. Almo is an employee/paid consultant for, reports receiving commercial research grants from, and holds ownership interest (including patents) in Cue Biopharma. No potential conflicts of interest were disclosed by the other authors.

Authors' Contributions

Conception and design: S.N. Quayle, N. Girgis, Z. Merazga, S. Hulot, A. Nelson, J.F. Ross, P.A. Kiener, S. Almo, R. Chaparro, R. Seidel, A. Suri, S. Cemerski, K.J. Pienta, M.E. Simcox

Development of methodology: N. Girgis, D.R. Thapa, Z. Merazga, S. Hulot, A. Nelson, D.R. Beal, E. Spaulding, S. Almo, K.J. Pienta

Acquisition of data (provided animals, acquired and managed patients, provided facilities, etc.): N. Girgis, D.R. Thapa, Z. Merazga, M.M. Kemp, A. Histed, F. Zhao, M. Moreta, P. Ruthardt, S. Hulot, A. Nelson, L.D. Kraemer, L. Witt, J. Ryabin, J. Soriano, M. Haydock, E. Spaulding, S. Cemerski

Analysis and interpretation of data (e.g., statistical analysis, biostatistics, computational analysis): S.N. Quayle, N. Girgis, D.R. Thapa, Z. Merazga, M.M. Kemp, A. Histed, F. Zhao, M. Moreta, P. Ruthardt, S. Hulot, A. Nelson, L.D. Kraemer, D.R. Beal, L. Witt, J. Ryabin, J. Soriano, E. Spaulding, P.A. Kiener, S. Cemerski, K.J. Pienta

Writing, review, and/or revision of the manuscript: S.N. Quayle, N. Girgis, D.R. Thapa, Z. Merazga, M.M. Kemp, A. Histed, F. Zhao, M. Moreta, P. Ruthardt, S. Hulot, D.R. Beal, J.F. Ross, P.A. Kiener, S. Almo, R. Chaparro, A. Suri, S. Cemerski, K.J. Pienta, M.E. Simcox

Administrative, technical, or material support (i.e., reporting or organizing data, constructing databases): S.N. Quayle, N. Girgis, Z. Merazga, M. Moreta, S. Hulot, L.D. Kraemer, L. Witt, J. Soriano, S. Cemerski

Study supervision: S.N. Quayle, N. Girgis, M. Moreta, J.F. Ross, P.A. Kiener, A. Suri, S. Cemerski

The costs of publication of this article were defrayed in part by the payment of page charges. This article must therefore be hereby marked *advertisement* in accordance with 18 U.S.C. Section 1734 solely to indicate this fact.

Received October 14, 2019; revised December 5, 2019; accepted January 13, 2020; published first January 21, 2020.

References

1. Trottier H, Franco EL. Human papillomavirus and cervical cancer: burden of illness and basis for prevention. Am J Manag Care 2006;12: S462–72.
2. Forman D, de Martel C, Lacey CJ, Soerjomataram I, Lortet-Tieulent J, Bruni L, et al. Global burden of human papillomavirus and related diseases. Vaccine 2012; 30S:F12–23.
3. Chaturvedi AK, Engels EA, Pfeiffer RM, Hernandez BY, Xiao W, Kim E, et al. Human papillomavirus and rising oropharyngeal cancer incidence in the United States. J Clin Oncol 2011;29:4294–301.
4. Berman TA, Schiller JT.Human papillomavirus in cervical cancer and oropharyngeal cancer: one cause, two diseases. Cancer 2017;123:2219–29.
5. Trimble CL, Morrow MP, Kraynyak KA, Shen X, Dallas M, Yan J, et al. Safety, efficacy, and immunogenicity of VGX-3100, a therapeutic synthetic DNA vaccine targeting human papillomavirus 16 and 18 E6 and E7 proteins for cervical intraepithelial neoplasia 2/3: a randomized, double-blind, placebo-controlled phase 2b trial. Lancet 2015;386:2078–88.
6. Stevanović S, Draper LM, Langhan MM, Campbell TE, Kwong ML, Wunderlich JR, et al. Complete regression of metastatic cervical cancer after treatment with human papillomavirus-targeted tumor-infiltrating T cells. J Clin Oncol 2015;33:1543–50.
7. Stevanović S, Pasetto A, Helman SR, Gartner JJ, Prickett TD, Howie B, et al. Landscape of immunogenic tumor antigens in successful immunotherapy of virally induced epithelial cancer. Science 2017;356:200–5.

8. Doran SL, Stevanović S, Adhikary S, Gartner JJ, Jia L, Kwong MLM, et al. T-cell receptor gene therapy for human papillomavirus-associated epithelial cancers: a first-in-human, phase I/II study. J Clin Oncol 2019;37:2759–68.
9. Mirabello L, Yeager M, Yu K, Clifford GM, Xiao Y, Zhu B, et al. HPV16 E7 genetic conservation is critical to carcinogenesis. Cell 2017;170:1164–74.
10. Ressing ME, Sette A, Brandt RMP, Ruppert J, Wentworth PA, Hartman M, et al. Human CTL epitopes encoded by human papillomavirus type 16 E6 and E7 identified through in vivo and in vitro immunogenicity studies of HLA-A*0201-binding peptides. J Immunol 1995;154:5934–43.
11. Riemer AB, Keskin DB, Zhang G, Handley M, Anderson KS, Brusic V, et al. A conserved E7-derived cytotoxic T lymphocyte epitope expressed on human papillomavirus 16-transformed HLA-A2$^+$ epithelial cancers. J Biol Chem 2010; 285:29608–22.
12. Gonzalez-Galarza FF, Christmas S, Middleton D, Jones AR. Allele frequency net: a database and online repository for immune gene frequencies in worldwide populations. Nucleic Acids Res 2011;39:D913–19.
13. Van Meir H, Kenter GG, Burggraaf J, Kroep JR, Welters MJ, Melief CJ, et al. The need for improvement of the treatment of advanced and metastatic cervical cancer, the rationale for combined chemo-immunotherapy. Anticancer Agents Med Chem 2014;14:190–203.
14. Tewari KS, Monk BJ.New strategies in advanced cervical cancer: from angiogenesis blockade to immunotherapy. Clin Cancer Res 2014;20:5349–58.
15. Sun YY, Peng S, Han L, Qiu J, Song L, Tsai Y, et al. Local HPV recombinant vaccinia boost following priming with an HPV DNA vaccine enhances local HPV-specific CD8+ T-cell-mediated tumor control in the genital tract. Clin Cancer Res 2016;22:657–69.
16. Kenter GG, Welters MJ, Valentijn AR, Lowik MJ, Berens-van der Meer DM, Vloon AP, et al. Phase I immunotherapeutic trial with long peptides spanning the E6 and E7 sequences of high-risk human papillomavirus 16 in end-stage cervical cancer patients shows low toxicity and robust immunogenicity. Clin Cancer Res 2008;14:169–77.
17. Hahnefeld C, Drewianka S, Herberg FW. Determination of kinetic data using surface plasmon resonance biosensors. Methods Mol Med 2004;94:299–320.
18. Jin BY, Campbell TE, Draper LM, Stevanović S, Weissbrich B, Yu Z, et al. Engineered T cells targeting E7 mediate regression of human papillomavirus cancers in a murine model. JCI Insight 2018;3:e99488.
19. Hezareh M, Hessell AJ, Jensen RC, van de Winkel JGJ, Parren PWHI. Effector function activities of a panel of mutants of a broadly neutralizing antibody against human immunodeficiency virus type 1. J Virol 2001;75:12161–68.
20. Brodsky FM, Parham P. Monomorphic anti-HLA-A,B,C monoclonal antibodies detecting molecular subunits and combinatorial determinants. J Immunol 1982; 128:129–35.
21. Ladasky JJ, Shum BP, Canavez F, Seuánez HN, Parham P. Residue 3 of β_2-microglobulin affects binding of class I MHC molecules by the W6/32 antibody. Immunogenetics 1999;49:312–20.
22. Heaton KM, Ju G, Grimm EA. Human interleukin 2 analogues that preferentially bind the intermediate-affinity Interleukin 2 receptor lead to reduced secondary cytokine secretion: implications for the use of these interleukin 2 analogues in cancer immunotherapy. Cancer Res 1993;53:2597–602.
23. Stauber DJ, Debler EW, Horton PA, Smith KA, Wilson IA. Crystal structure of the IL-2 signaling complex: paradigm for a heterotrimeric cytokine receptor. Proc Natl Acad Sci U S A 2006;103:2788–93.
24. Brownlie RJ, Zamoyska R. T cell receptor signalling networks: branched, diversified and bounded. Nat Rev Immunol 2013;13:257–69.
25. Rocha-Zavaleta L, Huitron C, Cacéres-Cortés JR, Alvarado-Moreno JA, Valle-Mendiola A, Soto-Cruz I, et al. Interleukin-2 (IL-2) receptor-$\beta\gamma$ signalling is activated by c-Kit in the absence of IL-2, or by exogenous IL-2 via JAK3/STAT5 in human papillomavirus-associated cervical cancer. Cell Signal 2004; 16:1239–47.
26. Newberg MH, Smith DH, Haertel SB, Vining DR, Lacy E, Engelhard VH. Importance of MHC class 1 α2 and α3 domains in the recognition of self and non-self MHC molecules. J Immunol 1996;156:2473–80.
27. Rosenberg SA, Mulé JJ, Spiess PJ, Reichert CM, Schwarz SL. Regression of established pulmonary metastases and subcutaneous tumor mediated by the systemic administration of high-dose recombinant interleukin 2. J Exp Med 1985;161:1169–88.
28. Gérard CM, Baudson N, Kraemer K, Ledent C, Pardoll D, Bruck C. Recombinant human papillomavirus type 16 E7 protein as a model antigen to study the vaccine potential in control and E7 transgenic mice. Clin Cancer Res 2001;7:838s-47s.
29. Mkrtichyan M, Chong N, Eid RA, Wallecha A, Singh R, Rothman J, et al. Anti-PD-1 antibody significantly increases therapeutic efficacy of Listeria monocytogenes (Lm)-LLO immunotherapy. J Immunother Cancer 2013;1:15.
30. Luo M, Wang H, Wang Z, Cai H, Lu Z, Li Y, et al. A STING-activating nanovaccine for cancer immunotherapy. Nat Nanotechnol 2017;12:648–54.
31. Tran E, Robbins PF, Lu YC, Prickett TD, Gartner JJ, Jia L, et al. T-cell transfer therapy targeting mutant KRAS in cancer. N Engl J Med 2016;375: 2255–62.
32. Zacharakis N, Chinnasamy H, Black M, Xu H, Lu YC, Zheng Z, et al. Immune recognition of somatic mutations leading to complete durable regression in metastatic breast cancer. Nat Med 2018;24:724–30.
33. Morgan RA, Dudley ME, Wunderlich JR, Hughes MS, Yang JC, Sherry RM, et al. Cancer regression in patients after transfer of genetically engineered lymphocytes. Science 2006;314:126–29.
34. Atkins MB, Lotze MT, Dutcher JP, Fisher RI, Weiss G, Margolin K, et al. High-dose recombinant Interleukin 2 therapy for patients with metastatic melanoma: analysis of 270 patients treated between 1985 and 1993. J Clin Oncol 1999;17: 2105–16.
35. Dutcher JP, Schwartzentruber DJ, Kaufman HL, Agarwala SS, Tarhini AA, Lowder JN, et al. High dose interleukin-2 (aldesleukin) – expert consensus on best management practices-2014. J Immunother Cancer 2014;2:26.
36. Amaria R, Reuben A, Cooper Z, Wargo JA. Update on use of aldesleukin for treatment of high-risk metastatic melanoma. Immunotargets Ther 2015;4:79–89.
37. Quandt J, Schlude C, Bartoschek M, Will R, Cid-Arregui A, Schölch S, et al. Long-peptide vaccination with driver gene mutations in p53 and Kras induces cancer mutation-specific effector as well as regulatory T cell responses. Oncoimmunology 2018;7:e11500671.
38. Agata Y, Kawasaki A, Nishimura H, Ishida Y, Tsubata T, Yagita H, et al. Expression of the PD-1 antigen on the surface of stimulated mouse T and B lymphocytes. Intl Immunol 1996;8:765–72.
39. Massarelli E, William W, Johnson F, Kies M, Ferrarotto R, Guo M, et al. Combining immune checkpoint blockade and tumor-specific vaccine for patients with incurable human papillomavirus 16-related cancer: a phase 2 clinical trial. JAMA Oncol 2019;5:67–73.